

Structure formation in the presence of dark energy perturbations

L. R. Abramo¹, R. C. Batista¹, L. Liberato² and R. Rosenfeld²

¹ Instituto de Física, Universidade de São Paulo
CP 66318, 05315-970, São Paulo, Brazil

² Instituto de Física Teórica, Universidade Estadual Paulista
R. Pamplona 145, 01405-900, São Paulo, Brazil

E-mail: abramo@fma.if.usp.br, rbatista@fma.if.usp.br,
liberato@ift.unesp.br, rosenfel@ift.unesp.br

February 1, 2008

Abstract. We study non-linear structure formation in the presence of dark energy. The influence of dark energy on the growth of large-scale cosmological structures is exerted both through its background effect on the expansion rate, and through its perturbations as well. In order to compute the rate of formation of massive objects we employ the Spherical Collapse formalism, which we generalize to include fluids with pressure. We show that the resulting non-linear evolution equations are identical to the ones obtained in the Pseudo-Newtonian approach to cosmological perturbations, in the regime where an equation of state serves to describe both the background pressure relative to density, and the pressure perturbations relative to the density perturbations as well. We then consider a wide range of constant and time-dependent equations of state (including phantom models) parametrized in a standard way, and study their impact on the non-linear growth of structure. The main effect is the formation of dark energy structure associated with the dark matter halo: non-phantom equations of state induce the formation of a dark energy halo, damping the growth of structures; phantom models, on the other hand, generate dark energy voids, enhancing structure growth. Finally, we employ the Press-Schechter formalism to compute how dark energy affects the number of massive objects as a function of redshift (number counts.)

Keywords: Cosmology: theory — Cosmology: large-scale structure of the Universe

1. Introduction

Observations of high-redshift SNIa imply that the expansion of the universe has been accelerating in the past few billions of years [1, 2, 3, 4]. This is corroborated by at least three broadly independent observations: the angular spectrum of the cosmic microwave background temperature fluctuations [5, 6], the galaxy-galaxy correlation function, which traces the spatial distribution of large-scale structure [7, 8], and the baryon acoustic oscillations [9]. Presently, the combined datasets favour a flat universe with $\Omega_m \simeq 0.27$, where the remaining 73% of the energy budget is taken up by dark energy.

These observations suggest that the dominant contribution to the present energy density of the Universe can be described by a dark (*i.e.*, weakly or non-interacting) fluid with equation of state (EoS) $w_{de} = p_{de}/\rho_{de} < -1/3$. A particular case of such a substance would be the cosmological constant, Λ , for which $w_\Lambda = -1$. Many other models with $w_{de} \neq -1$ have been proposed, usually in the framework of a scalar field ("quintessence") or some other form of cosmic fluid with negative pressure – see, e.g., [10] for a comprehensive review.

A more direct approach to the phenomenology of dark energy has been recently adopted, in which the equation of state w_{de} is expressed in terms of a certain parametrization with respect to its time dependence [11, 12, 13, 14]. Although determining the equation of state as a function of redshift would probably not help to reveal the nature of dark energy, it could go a long way towards discriminating among existing models. Hence, one of the most important tasks ahead for observational cosmology is to gather sufficient data to successfully and unequivocally distinguish between this landscape of possibilities. As for theorists, the challenge is to determine in which additional ways dark energy may manifest itself in nature, apart from the acceleration of the overall expansion rate of the Universe.

One of the ways in which dark energy changes the evolution of our local Universe is through its influence over the rates of formation and growth of collapsed structures (halos). Since all galaxies and quasars, as well as supernovae and putative sources of gamma-ray bursts, lie inside collapsed structures of some type or another, their distribution in size, space and in time will reflect to some extent the influence of dark energy.

There are basically three mechanisms through which dark energy affects large-scale structure. First, the collapse of an overdense region due to gravitational instability is slowed down by the Hubble expansion drag, so any additional component which increases the expansion rate for the same value of the energy density will dampen the formation of collapsed structures. Second, as the accelerated expansion picks up speed, the large-scale gravitational potentials grow slower, then start to decay. This means that, as dark energy becomes the dominating dynamical component of the Universe, some large-scale overdensities will grow slower, and the process of gravitational collapse will even reverse itself at scales comparable to the Hubble horizon. And third, if dark

energy is not the cosmological constant then it must fluctuate both in time and in space. Hence, dark energy not only feels the gravitational pull of a matter halo, but it tends to form halos itself, thus influencing back those matter halos in a non-linear manner. Notice that the first two mechanisms affect collapsed structures only indirectly, through changes in the Hubble expansion rate, while the third mechanism depends on the clustering properties of dark energy. Since different models of dark energy can easily produce the same homogeneous expansion rate, but they hardly ever produce the same perturbations, the largest potential to probe the nature of dark energy possibly comes from such perturbative mechanisms.

In a previous paper, two of the present authors have studied the influence at the background level (no dark energy fluctuations) of different parametrizations of the dark energy equation of state (EoS) in the evolution of dark matter perturbations and in the final number counts of dark matter halos [15]. Our main purpose in this paper is to extend this analysis by studying non-linear structure formation including the possibility of dark energy fluctuations.

Related approaches were recently developed by Nunes & Mota [16], Manera & Mota [17], Nunes, Silva & Aghanim [18] and Dutta & Maor [19], but those works considered scalar field dark energy. Here we focus instead on dark energy as described by some parametrization for the EoS as a function of redshift. This is more general than the scalar field approach, since the EoS is directly related to the physical observables most widely used to measure cosmic acceleration. Moreover, in contrast to [16, 17], we were able to investigate the non-linear regime of both dark matter and dark energy clustering consistently, and we have found that it has an important effect on the formation of massive objects ($M > 10^{13} M_{\odot}$). Although the description of dark energy entirely in terms of its EoS may be too restrictive, the present work proves that the impact of dark energy perturbations on the formation of collapsed objects is both substantial and observable.

This paper is organized as follows. In Sec. 2 we extend the traditional Spherical Collapse (SC) model, originally used only to describe gravitational collapse in the absence of pressure, to incorporate the possibility of coupled perturbations in 2 fluids, namely pressureless dark matter and negative pressure dark energy. We verify this generalization showing under what conditions the SC model is equivalent to a Pseudo-Newtonian (PN) perturbation theory approach. In Sec. 3 we study the linear evolution of the generalized SC equations, and the effects of dark energy on the formation and on the initial stages of the evolution of matter halos. In Sec. 4 we analyze the fully non-linear system of SC equations, and how the formation of strongly non-linear (collapsed) matter halos both affects and is affected by dark energy halos. In Sec. 5 we show how our results can be included in a Press-Schechter formalism in order to derive the consequences to dark matter halos number counts. We conclude in Sec. 6.

2. The spherical collapse model and its generalizations

The simplest (semi-) analytical tool to study non-linear structure formation is the SC model [20]. It has been shown that the SC equations can be actually derived from General Relativity, as long as shear does not play a significant role [21].

Most studies about the impact of dark energy on structure formation were performed under the assumption that dark energy is uniformly distributed. In this case, where dark energy affects only background quantities, the SC model can be easily modified to incorporate dark energy effects. For instance, the abundance of rich clusters of galaxies estimated within the SC model was used to constrain the cosmological model and the properties of dark energy fluid in the context of the simplest case of a cosmological constant [22, 23], in the case of a constant $w_{\text{de}} \neq -1$ [24, 25, 26, 27, 28], as well as the case of dynamical dark energy models with some parametrizations of $w_{\text{de}}(t)$ [15].

However, the standard SC framework was originally designed to describe perturbations in pressureless matter, while we are interested in the effects of perturbations in an extra component whose pressure is very large and negative. If we want to study a gravitationally coupled system of matter (we do not distinguish between dark matter and baryons here) and dark energy, the SC model must be expanded beyond the realm of the Einstein-de Sitter model.

Consequences of dark energy fluctuations in the studies of structure formation are more naturally incorporated by introducing a scalar field with a suitable potential to model the dark energy component, such as the quintessence field. In this approach, the authors of Refs. [16, 17, 29, 30] proposed an extension of the SC equations that take into account fluctuations in the dark energy field for minimally and non-minimally coupled quintessence field.

It is often more convenient, and completely equivalent at the background level, to introduce a time-dependent parametrization for the dark energy EoS, $w_{\text{de}}(z)$. Since it is possible to reconstruct the scalar field potential from a general parametrization of dark energy, or directly from the EoS $w_{\text{de}}(z)$ [31, 32], the two approaches are in fact closely related. Our goal in this section is to generalize the SC model with a fluid description of dark energy in order to include the possibility of dark energy fluctuations.

We will check this generalized SC model with the results from the Pseudo-Newtonian (PN) approach to cosmology [33] for perfect fluids with pressure. The advantages of the PN framework are that it is both simpler than full-blown non-linear General Relativity (GR), and more intuitive. Crucially, it is in good agreement with GR in the linear regime [34, 35]. As we will see, the PN approach is also particularly useful if we want to keep contact with the description of dark energy in terms of a parametrization for its EoS, and it can be easily generalized to a multi-fluid system.

The only remaining question is whether the two approaches agree with each other. Next we verify under which conditions the SC model is equivalent to the PN approach.

2.1. Spherical Collapse

The continuity equation for a single perfect fluid j with background density ρ_j and pressure $p_j = w_j \rho_j$ is given by:

$$\dot{\rho}_j + 3H\rho_j(1 + w_j) = 0, \quad (1)$$

where $H = \dot{a}/a$ is the Hubble parameter. Consider now a spherically symmetric region of radius r and with a homogeneous density ρ_{c_j} (a top-hat distribution). Suppose that, at time t , $\rho_{c_j}(t) = \rho_j(t) + \delta\rho_j$. If $\delta\rho_j > 0$ this spherical region will eventually collapse from its own gravitational pull, otherwise it will expand faster than the average Hubble flow, generating what is known as a void. The evolution of such simplified spherical regions can be described in close analogy with the continuity Eq. (1), but now with $p_{c_j} = w_{c_j}\rho_{c_j}$:

$$\dot{\rho}_{c_j} + 3h\rho_{c_j}(1 + w_{c_j}) = 0, \quad (2)$$

where $h = \dot{r}/r$ denotes the local expansion rate inside the spherical region. Note that, in principle, we could have different equations of state inside and outside the spherical region, $w_{c_j} \neq w_j$. In fact, the difference between the local and the background equations of state $\delta w_j \equiv w_{c_j} - w_j$ can be related to the fluid's effective speed of sound, $c_{\text{eff}j}^2 = \delta p_j / \delta \rho_j$, through:

$$\delta w_j = \frac{\delta \rho_j}{\rho_j + \delta \rho_j} (c_{\text{eff}j}^2 - w_j). \quad (3)$$

Usually, c_{eff}^2 is regarded as a free parameter – although, rigorously, in perturbation theory the only other free parameter is the true sound speed of inhomogeneities, c_X^2 [36]. Here the sound speed c_{eff}^2 is defined as the ratio between two independent perturbative degrees of freedom, so not only it is gauge dependent, but it may depend also on the initial conditions for those perturbations. Therefore, c_{eff}^2 stands as a proxy for the pressure perturbations.

For simplicity, and in order to make contact with the PN equations, we will consider the case where the EoS is the same inside the collapsing sphere and in the background, so we take $\delta w_j = 0$ and thus $c_{\text{eff}j}^2 = w_j$. This situation can be readily obtained in cases such as a slow-rolling scalar field.

It should be noted that, in principle, there are instabilities in the growth of inhomogeneous perturbations whenever the sound speed becomes negative. However, within the spherical collapse model with a top-hat profile and the assumption of a space-independent c_{eff}^2 , there are no pressure or density gradients, so no such problem of instabilities arises.

By the same token as the first Friedmann equation, consider now the second Friedmann equation applied to the spherical region:

$$\frac{\ddot{r}}{r} = -\frac{4\pi G}{3} (\rho_c + 3p_c). \quad (4)$$

Notice that the density and pressure that appear in Eq. (4) are the sum of densities and pressures of *all* contributing fluids, while the continuity Eqs. (1)-(2) are valid for each individual fluid (in the absence, of course, of direct couplings between those fluids.)

It is useful to define the density contrast of a single fluid species j by the relation:

$$\delta_j + 1 = \frac{\rho_{c_j}}{\rho_j} . \quad (5)$$

Differentiating this with respect to time we obtain:

$$\dot{\delta}_j = 3(1 + \delta_j)(H - h)(1 + w_j) , \quad (6)$$

where we assumed $w_{c_j} = w_j$. Differentiating again with respect to time and employing the equations for the background and for the spherical region, we can derive the following non-linear evolution equation for δ_j :

$$\begin{aligned} \ddot{\delta}_j + \left(2H - \frac{\dot{w}_j}{1 + w_j} \right) \dot{\delta}_j - 4\pi G (1 + w_j) (1 + \delta_j) \sum_k \rho_k \delta_k (1 + 3w_k) = \\ \left[\frac{4 + 3w_j}{3(1 + w_j)} \right] \frac{\dot{\delta}_j^2}{1 + \delta_j} . \end{aligned} \quad (7)$$

Notice that we admit the possibility of a time-dependent EoS. For a system of n fluids, we must consider n equations such as (7), all coupled gravitationally through the term proportional to Newton's constant. Although they are not derived rigorously from General Relativity, we will see next that these equations find support in the PN approximation to gravitational interactions.

2.2. Pseudo-Newtonian Cosmology

Consider now the PN cosmological model, described by the equations [33]:

$$\frac{\partial \rho_j}{\partial t} + \vec{\nabla}_r \cdot (\vec{u}_j \rho_j) + p_j \vec{\nabla}_r \cdot \vec{u}_j = 0 , \quad (8)$$

$$\frac{\partial \vec{u}_j}{\partial t} + \left(\vec{u}_j \cdot \vec{\nabla}_r \right) \vec{u}_j = -\vec{\nabla}_r \Phi - \frac{\vec{\nabla}_r p_j}{\rho_j + p_j} , \quad (9)$$

$$\nabla_r^2 \Phi = 4\pi G \sum_k (\rho_k + 3p_k) , \quad (10)$$

where ρ_j , p_j , \vec{u}_j and Φ denote, respectively, the density, pressure, velocity and the Newtonian gravitational potential of the cosmic fluid. These equations are, respectively, generalizations of the continuity equation, of Euler's equation (both valid for each fluid species j), and of Poisson's equation (which is valid for the sum of all fluids.)

Cosmological perturbations are introduced by admitting inhomogeneous deviations away from the background quantities:

$$\rho_j = \rho_{0_j}(t) + \delta\rho_j(\vec{x}, t) , \quad (11)$$

$$p_j = p_{0_j}(t) + \delta p_j(\vec{x}, t) , \quad (12)$$

$$\vec{u}_j = \vec{u}_{0_j}(t) + \vec{v}_j(\vec{x}, t) , \quad (13)$$

$$\Phi = \Phi_0(t) + \phi(\vec{x}, t) . \quad (14)$$

Changing to comoving coordinates, $\vec{x} = \vec{r}/a$, (henceforth $\vec{\nabla}$ refers to gradient with respect to comoving coordinates \vec{x}) and using $\delta_j = \delta\rho_j/\rho_{0j}$, we find the following equations for the perturbed quantities:

$$\dot{\delta}_j + 3H(c_{\text{eff } j}^2 - w_j)\delta_j = -[1 + w_j + (1 + c_{\text{eff } j}^2)\delta_j] \frac{\vec{\nabla} \cdot \vec{v}_j}{a} - \frac{\vec{v}_j \cdot \vec{\nabla} \delta_j}{a} \quad (15)$$

$$\dot{\vec{v}}_j + H\vec{v}_j + \frac{\vec{v}_j \cdot \vec{\nabla}}{a} \vec{v}_j = -\frac{\vec{\nabla} \phi}{a} - \frac{c_{\text{eff } j}^2 \vec{\nabla} \delta}{a[1 + w_j + (1 + c_{\text{eff } j}^2)\delta_j]} , \quad (16)$$

$$\frac{\nabla^2 \phi}{a^2} = 4\pi G \sum_k \rho_{0k} \delta_k (1 + 3c_{\text{eff } k}^2) , \quad (17)$$

where $c_{\text{eff } j}^2 \equiv \delta p_j / \delta \rho_j$ is the effective sound speed of each fluid. In order to obtain these equations we have assumed that w_j and $c_{\text{eff } j}^2$ are functions of time only.

Notice that Eqs. (15)-(17) are valid even if δ_j is not small, so we can use them to follow the evolution of a collapsing region well into the non-linear regime. In fact, the PN equations of motion become a better approximation as the size of the system shrinks due to gravitational collapse. This is easy to see by noticing that in most collapsed regions of the Universe the density contrast δ_j may be extremely large, but the gravitational potentials are small, $\phi \ll 1$, and the local relative (peculiar) velocities are almost never relativistic. Hence, the PN equations may be a poor approximation at the moment of turnaround (when a spherical region breaks away from the Hubble flow) for the scales comparable to the Hubble horizon at the time of turnaround, but for all other scales and epochs it is a good approximation that becomes progressively better as the system collapses.

In order to simplify the PN equations, it is useful to define:

$$\theta_j \equiv \vec{\nabla} \cdot \vec{v}_j , \quad (18)$$

$$C_j \equiv a^{-1} \vec{\nabla} \cdot \left[(\vec{v}_j \cdot \vec{\nabla}) \vec{v}_j \right] , \quad (19)$$

and

$$f_j \equiv \vec{\nabla} \cdot \left[\frac{\vec{\nabla} \phi}{a} + \frac{c_{\text{eff } j}^2 \vec{\nabla} \delta_j}{a(1 + w_j + \delta_j + c_{\text{eff } j}^2 \delta_j)} \right] , \quad (20)$$

so that by taking the divergence of (16) we obtain:

$$\dot{\theta}_j + H\theta_j + C_j = -f_j . \quad (21)$$

We also define:

$$A_j \equiv 3H(c_{\text{eff } j}^2 - w_j)\delta_j , \quad (22)$$

$$B_j \equiv 1 + w_j + (1 + c_{\text{eff } j}^2)\delta_j , \quad (23)$$

and by neglecting the term $\vec{v}_j \cdot \vec{\nabla} \delta_j$, which is of order of v_j^2/c^2 , we can cast Eq. (15) in the form:

$$\dot{\delta}_j + A_j + \frac{\theta_j}{a} B_j = 0 . \quad (24)$$

Taking the partial derivative of (24) with respect to time, using Eq. (21) to eliminate $\dot{\theta}_j$ and Eq. (24) to eliminate θ_j we get:

$$\ddot{\delta}_j + \dot{A}_j + \left(A_j + \dot{\delta}_j\right) \left(2H - \frac{\dot{B}_j}{B_j}\right) - \frac{B_j}{a} (f_j + C_j) = 0. \quad (25)$$

In the appendix we explicitly show that, for a single fluid with $c_{eff}^2 = w = const$, PN and GR at the linear level differ only by a decaying mode.

Now we try to make contact with the SC equations. In order to reproduce Eq. (7) we must, first of all, assume that the velocity profile is consistent with the hypothesis of spherically symmetric collapse of a top-hat inhomogeneity, i.e., $\vec{v}_j = \theta(t)/3 \vec{x}$. Second, we also have to assume that $c_{eff,j}^2 = w_j$. Notice that because the intrinsic non-adiabatic pressure $\Gamma_j \sim \delta p_j - c_{s,j}^2 \delta \rho_j$, where the adiabatic sound speed is $c_{s,j}^2 = \frac{\dot{p}_j}{\dot{\rho}_j}$, our choice implies some amount of intrinsic entropy perturbations for the dark energy fluid.

With these choices we have: $A_j = 0$, $B_j = (1 + w_j)(1 + \delta_j)$ and $C_j = \theta_j^2/3a$. Notice that, with this velocity field, the LHS of equation (21) is identical to that of Raychaudhuri's equation when we assume that θ_j is a function of time only:

$$\dot{\theta}_j + H\theta_j + \frac{\theta_j^2}{3a} = -f_j. \quad (26)$$

This equation reduces to the one found in [21] if we neglect the gradients of the density contrast in f_j . Since we are considering the spherical collapse of a top-hat distribution (which is homogeneous inside the radius r), the terms including $\vec{\nabla}\delta_j$ which appear in f_j vanish. Under these conditions, Eq. (25) reduces to the equation for SC, Eq. (7).

It is interesting that in fact we were forced to assume both that $w_{c_j} = w_j$ in the SC formalism, and that $c_{eff,j}^2 = w_j$ in the PN formalism, in order that the two frameworks would result in identical equations. This is a further motivation for our choices of $\delta w_j = 0$ and $c_{eff,j}^2 = w_j$: only in this scenario we can trust that the physics of non-linear spherically symmetric collapse is well described by our dynamical equations. In order to describe a more general situation probably neither approach is suited, and one would be forced to resort to full-blown General Relativity. However it is possible that the numerical differences between SC and PN for other choices of δw_j and $c_{eff,j}^2$ are small.

2.3. Equations for non-linear spherical collapse in the presence of dark energy

We obtained non-linear differential equations that characterize the growth of spherically symmetric perturbations in fluids with arbitrary time-dependent equations of state. These equations are coupled through the gravitational interactions. We saw that both the PN and SC approaches agree with General Relativity for a pressureless fluid; furthermore, we have shown that they agree with each other in the case where $c_{eff,j}^2 = w_{c_j} = w_j$ and if the density profile is a top-hat ($\vec{\nabla}\delta_j = 0$.)

Particularizing to a model with only non-relativistic matter and dark energy, in which the latter is characterized solely by its EoS, the top-hat spherical regions evolve

according to a system of equations equivalent to (7):

$$\ddot{\delta}_m + 2H\dot{\delta}_m - \frac{4\dot{\delta}_m^2}{3(1+\delta_m)} = \frac{3H^2}{2}(1+\delta_m)[\Omega_m\delta_m + \Omega_{de}\delta_{de}(1+3w_{de})] , \quad (27)$$

$$\begin{aligned} \ddot{\delta}_{de} + \left(2H - \frac{\dot{w}_{de}}{1+w_{de}}\right)\dot{\delta}_{de} - \left[\frac{4+3w_{de}}{3(1+w_{de})}\right]\frac{\dot{\delta}_{de}^2}{1+\delta_{de}} = \\ \frac{3H^2}{2}(1+w_{de})(1+\delta_{de})[\Omega_m\delta_m + \Omega_{de}\delta_{de}(1+3w_{de})] , \end{aligned} \quad (28)$$

where δ_m is the density contrast in matter and δ_{de} is the density contrast in the dark energy component. These are the equations we will study in the following sections.

3. Solutions in linear regime

The linear regime of cosmological perturbations is valid for all scales during the radiation era, and for most scales during the matter era up until very recently. The initial stages of the process of gravitational collapse are indeed very well described by the linear regime for all but the smallest scales. Since this is a simple system which can be studied almost entirely with analytical tools, it is useful to try and extract some physics from Eqs. (27)-(28) while they are still in the linear regime. Neglecting the $\mathcal{O}(\delta^2)$ terms we obtain:

$$\ddot{\delta}_m + 2H\dot{\delta}_m = \frac{3H^2}{2}[\Omega_m\delta_m + \Omega_{de}\delta_{de}(1+3w_{de})] , \quad (29)$$

$$\begin{aligned} \ddot{\delta}_{de} + \left(2H - \frac{\dot{w}_{de}}{1+w_{de}}\right)\dot{\delta}_{de} \\ = \frac{3H^2}{2}(1+w_{de})[\Omega_m\delta_m + \Omega_{de}\delta_{de}(1+3w_{de})] . \end{aligned} \quad (30)$$

In principle, we can employ any given parametrization for dark energy as a function of time or redshift, but in order to find closed analytical formulas we initially take $w_{de} = \text{constant}$. We start by solving Eqs. (29)-(30) well inside the matter-dominated period ($z = 10^3$), when it is a good approximation to assume that $\Omega_{de} \approx 0$ and $\Omega_m \approx 1$. Changing the time variable to the scale factor a , the equations become:

$$\delta_m'' + \frac{3}{2}\frac{\delta_m'}{a} - \frac{3}{2a^2}\delta_m = 0 , \quad (31)$$

$$\delta_{de}'' + \frac{3}{2}\frac{\delta_{de}'}{a} - \frac{3}{2a^2}(1+w_{de})\delta_m = 0 , \quad (32)$$

where a prime denotes derivative with respect to a .

As is widely known, in this case the solution for the matter density contrast is $\delta_m(a) = C_1 a + C_2 a^{-3/2}$, where C_1 and C_2 are arbitrary constants. Neglecting the decaying mode of the matter density contrast, Eq. (32) then has the solution:

$$\delta_{de} = C_1(1+w_{de})a + C_3 = (1+w_{de})\delta_m + C_3 . \quad (33)$$

It is interesting to note that the adiabatic condition is $\delta_{de} = (1+w_{de})\delta_m$. Hence, any value $C_3 \neq 0$ implies a non-adiabatic initial condition – i.e., in such a case

the perturbations have an isocurvature component. However, local non-adiabatic perturbations are unstable, since they correspond to pressure gradients between the internal and external parts of the spherical region. These pressure gradients must eventually cancel out, so any non-adiabatic component must decay during the evolution of the perturbations, leaving only the usual adiabatic (curvature) fluctuations.

Notice that the condition of adiabaticity is different in the usual dark energy models ($w_{\text{de}} > -1$) compared to phantom models ($w_{\text{de}} < -1$): for phantom models, adiabatic initial conditions mean that any initial overdensity in matter is matched by an underdensity in dark energy, and vice-versa. So, for example, take a phantom dark energy model and a positive density perturbation in dark matter. If initially the dark energy perturbation is also positive, then the pressure gradients will cause the dark energy halo to decay, then to turn it into a void, thus switching the sign of the dark energy perturbation – see [29] for a similar switching effect.

The effect of dark energy perturbations on the evolution of dark matter perturbations is easily understood from Eq. (29): dark energy perturbations become a source for dark matter perturbation. Since $(1 + 3w_{\text{de}}) < 0$, a dark energy overdensity decreases dark matter clustering, which is intuitive since a local concentration of dark energy would speed up the acceleration in that region. The opposite holds for a region with a dark energy underdensity. We show some examples in the next subsections. For the remainder of the paper we adopt $\Omega_m = 0.25$, $\Omega_{\text{de}} = 0.75$ and $h_0 = 0.72$.

3.1. Constant w_{de} : non-phantom models

In the case of non-phantom dark energy we have $1 + w_{\text{de}} > 0$, and therefore Eq. (33) implies that a region containing a matter overdensity ($\delta_m > 0$) induces a dark energy overdensity ($\delta_{\text{de}} > 0$) in that same region. Conversely, a matter underdensity region ($\delta_m < 0$) induces a dark energy underdensity ($\delta_{\text{de}} < 0$). Hence, in the non-phantom case a halo of dark matter induces a halo of dark energy, and a void of dark matter induces a void of dark energy. This behaviour is generic if we limit the scope of initial conditions to adiabatic perturbations – as predicted by inflation and confirmed by WMAP [6].

In order to study the impact of dark energy fluctuations on the growth of dark matter perturbations we show in Fig. 1 the evolution of δ_m with and without the inclusion of dark energy fluctuations, for two different values of the EoS: $w_{\text{de}} = -0.9$ and -0.8 . We use adiabatic initial conditions at $z_i = 1000$, with $\delta'_m(z_i) = -\delta_m(z_i)/(1 + z_i)$.

The initial condition on the derivative of the density perturbation comes from the assumption that dark energy is negligible initially. As the figure shows, the inclusion of dark energy perturbations actually suppresses the growth of dark matter perturbations in this case. The differences in the linear regime are roughly proportional to $1 + w_{\text{de}}$. In this same figure we also show the growth of the dark energy perturbation, which is much smaller than the matter fluctuation, as expected, but also tends to form a dark energy halo.

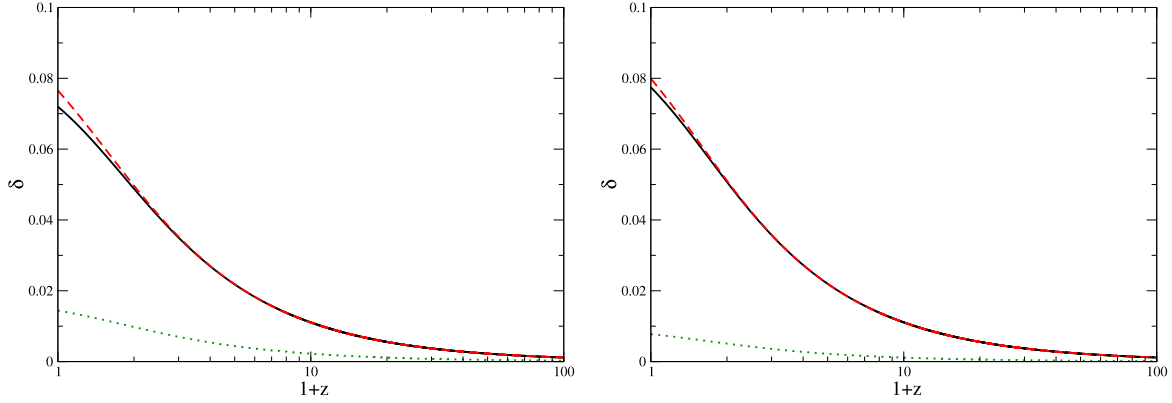


Figure 1. Growth of matter perturbation with (solid lines) and without (dashed lines) dark energy perturbations together with growth of dark energy perturbations (dotted lines) for $w_{\text{de}} = -0.8$ (left panel) and $w_{\text{de}} = -0.9$ (right panel).

3.2. Constant w_{de} : phantom models

In the case of phantom dark energy we have $1 + w_{\text{de}} < 0$, and therefore Eq. (33) implies that a matter overdensity region ($\delta_{\text{m}} > 0$), which will later become a dark matter halo, induces a dark energy density void ($\delta_{\text{de}} < 0$), and vice-versa. Again, this behaviour is generic for purely adiabatic initial conditions.

In Fig. 2 we show the effects of dark energy fluctuations on the growth of dark matter perturbations for two different values of the EoS, $w_{\text{de}} = -1.1$ and -1.2 . As in the case of non-phantom dark energy, the differences are small and increase with larger values of $|1 + w_{\text{de}}|$. However, contrary to the non-phantom case, fluctuations in phantom dark energy enhance the growth of dark matter perturbations. We also show the growth of the dark energy perturbation which, as expected, tends to form a dark energy void.

3.3. Varying w_{de}

In the framework of single scalar field descriptions of dark energy it is impossible for the EoS to cross the so-called phantom barrier at $w_{\text{de}} = -1$ [37]. However, in our phenomenological approach we could in principle have a time-varying parametrization of $w_{\text{de}}(z)$ crossing the phantom barrier. In fact, this is the case with many parametrizations adjusted to fit SNIa data [14].

The existence of a phantom barrier is hinted in our approach by the presence of the term $\dot{w}_{\text{de}}(1 + w_{\text{de}})^{-1}$ in Eq. (30). Although the divergence at $w_{\text{de}} = -1$ is not necessarily fatal for the solutions of the differential equations, here we consider only dark energy parametrizations that are phantom or non-phantom during all times.

We will study a parametrization of the dark energy EoS of the form [38]:

$$w_{\text{de}} = w_0 + w_1(1 - a) = w_0 + w_1 \frac{z}{1 + z}, \quad (34)$$

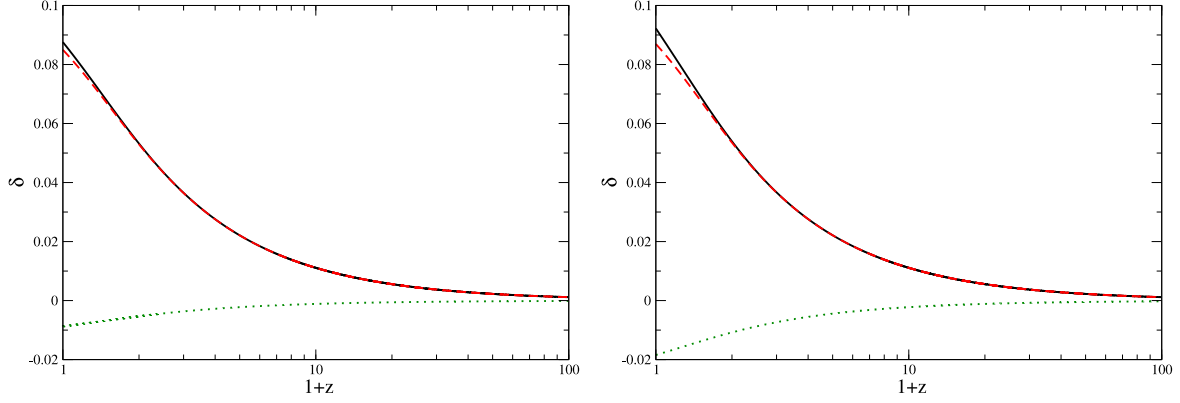


Figure 2. Growth of matter perturbation with (solid lines) and without (dashed lines) dark energy perturbations together with growth of dark energy perturbations (dotted lines) for $w_{\text{de}} = -1.1$ (left panel) and $w_{\text{de}} = -1.2$ (right panel).

and we choose parameters w_0 and w_1 which are consistent with the 2σ regions which are jointly constrained by observations of the CMB, supernovas and baryon oscillations – see, for instance, [39, 40].

In Fig. 3 we show the impact of dark energy flucutations for a variable EoS for both phantom and non-phantom cases. The results are similar to the constant EoS cases.

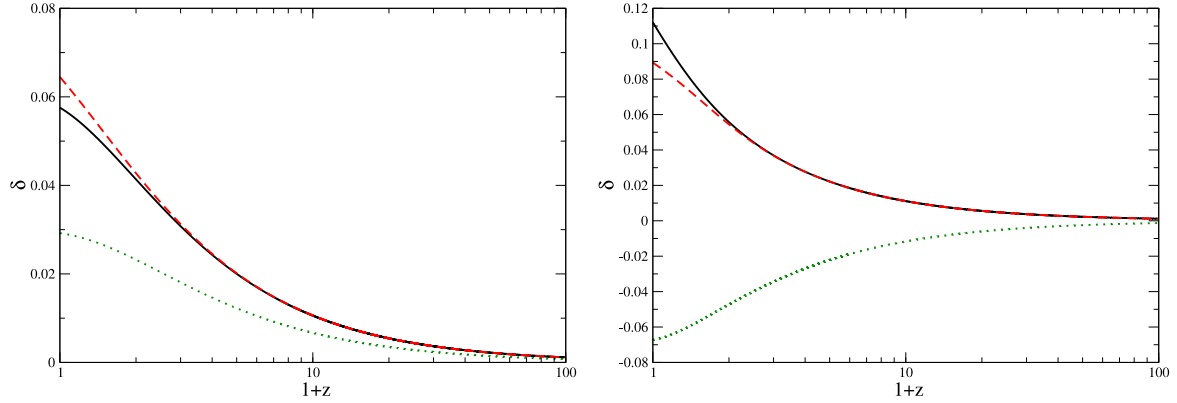


Figure 3. Evolution of $\delta_m(z)$ in linear regime with dark energy adiabatic IC with $w_0 = -0.75$ and $w_1 = 0.4$ (non-phantom, left figure) and with $w_0 = -1.1$ and $w_1 = -1$ (phantom, right figure) including dark energy perturbations (full line) and without dark energy perturbations (dashed line). The growth of dark energy perturbations (dotted line) is also included.

4. Non-linear regime

In the non-linear regime, as in the linear regime, we consider again only models that are phantom or non-phantom at all times. We solve Eqs. (27)-(28), and for brevity's sake we limit our scope to the parametrizations discussed in subsection 3.3: $(w_0, w_1) = (-0.75, 0.4)$ and $(-1.1, -1)$. In particular, we are interested in the impact of the dark energy fluctuations on the collapse of dark matter structures. We will see that the effects found in the linear case (of the order of a few percent) are amplified by the non-linear evolution.

In Fig. 4 (left panel) we show the dark matter density contrast for initial conditions chosen such that the collapse (indicated by the divergence of the density contrast) of a spherical dark matter structure happens at the present time ($z = 0$). Physically, this would correspond to the formation of an object such as a supercluster. Dark energy fluctuations have a dramatic effect in this case: in the non-phantom case, that structure would have collapsed much earlier if the dark energy fluctuations had not been taken into account. In the right panel of Fig. 4 we also show a phantom parametrization, where initial conditions are chosen such that the collapse of the dark matter structure takes place today without dark energy perturbations. In this case, the inclusion of dark energy perturbations enhances the clustering of dark matter and cause that same structure to collapse earlier.

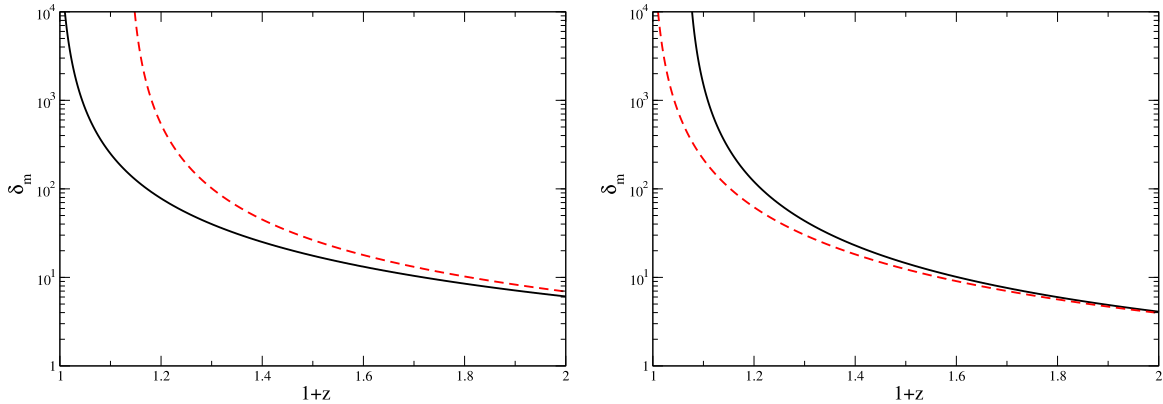


Figure 4. Non-linear evolution of $\delta_m(z)$ for dark matter with (solid) and without (dashed) dark energy perturbation for the case of a non-phantom (left panel) and a phantom (right panel) parametrization. In the left panel, initial conditions are chosen such that dark matter with dark energy perturbations collapses today ($z = 0$), whereas in the right panel initial conditions are chosen such that dark matter without dark energy perturbations collapses today.

In Fig. 5 we contrast the evolution of the non-linear densities in dark matter and dark energy against the evolution of the linearized densities. In that figure the initial conditions are chosen such that the non-linear dark matter perturbation diverges at $z = 0$. Hence, the value of the linearized dark matter perturbation at $z = 0$ in this case

corresponds to the definition of the critical density contrast for that redshift, $\delta_c(z=0)$. In the next Section we will employ the critical density contrast as a function of redshift in order to compute the Press-Schechter function.

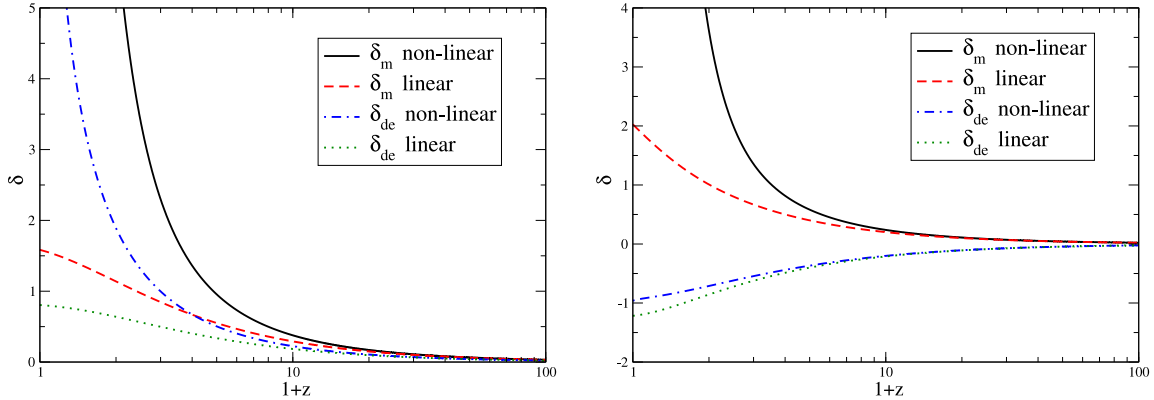


Figure 5. Non-linear evolution of $\delta(z)$ for dark matter (solid line) and dark energy (dot-dashed line). The initial conditions are chosen such that dark matter collapses today ($z=0$). Also shown are the linearized evolution of dark matter (dashed line) and dark energy (dotted line) perturbations. The left and right panels correspond to the parametrizations $(w_0, w_1) = (-0.75, 0.4)$ (left panel) and $(-1.1, -1)$ (right panel.)

5. Number Counts of Dark Matter Halos

We will use the Press-Schechter approach [41] in order to estimate the number counts of dark matter halos for different bins of redshifts and halo masses. More realistic mass functions could be used (see, for instance, [42]) but our intention here is simply to point out how number counts differ in scenarios with dark energy compared to the standard Λ CDM model. We believe these differences would be essentially the same in more sophisticated models of nonlinear structure formation, such as the model of ellipsoidal collapse.

The Press-Schechter formalism assumes that the fraction of mass in the universe contained in gravitationally bound systems with masses greater than M is given by the fraction of space where the linearly evolved density contrast exceeds a threshold δ_c , and that the density contrast is normally distributed with zero mean and variance $\sigma^2(M)$ – the root-mean-square value of the density contrast δ at scales containing a mass M . Therefore, it is assumed that for a massive sphere to undergo gravitational collapse at a redshift z , its *linear* overdensity should exceed a certain threshold δ_c , defined as the linearly evolved density contrast at the instant when the non-linear density contrast associated with the mass M diverges (*i.e.*, at the moment of collapse.) Since each scale M collapses at a given redshift (bigger masses, corresponding to larger scales, collapse

later), the critical density contrast is a function of redshift, $\delta_c = \delta_c(z)$. Nevertheless, notice that only linear quantities are used in this formalism. For a review of the Press-Schechter formalism see, for instance, [43].

In order to illustrate how dark energy affects gravitational collapse, in Fig. 6 we show $\delta_c(z)$ in a few dark energy scenarios. Notice that the inclusion of dark energy perturbations has a dramatic effect in $\delta_c(z)$, with a substantial suppression in the non-phantom case and a substantial enhancement in the phantom case. If dark energy perturbations are not included we reproduce the results of [15].

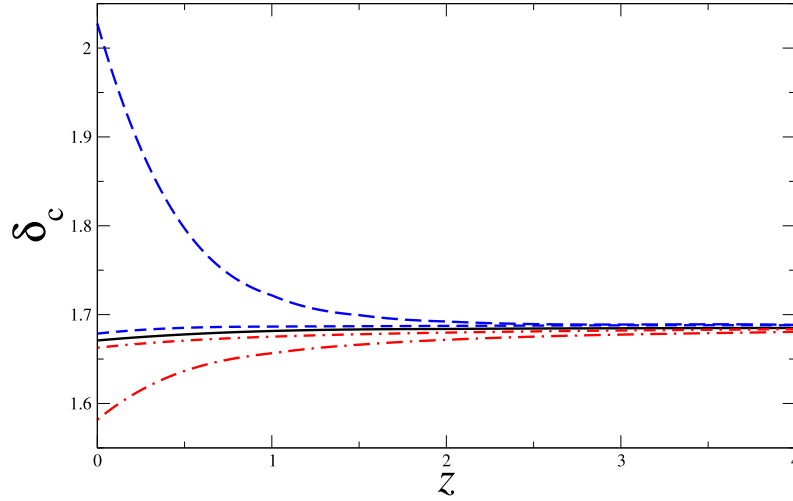


Figure 6. Values of the linear critical density contrast δ_c as a function of the collapse redshift. The solid line is the usual Λ CDM result. The values which do not include dark energy perturbations are shown for phantom (dashed line) and non-phantom (dot-dashed line) cases. The values with dark energy perturbations are shown for phantom (long dashed line) and non-phantom (long dot-dashed line). The non-phantom and phantom cases correspond to the same parametrizations used in Fig. 3.

These assumptions lead to the well-known analytical formula for the comoving number density of collapsed halos of mass in the range M and $M + dM$ at a given redshift z :

$$\frac{dn}{dM}(M, z) = -\sqrt{\frac{2}{\pi}} \frac{\rho_{m0}}{M} \frac{\delta_c(z)}{\sigma(M, z)} \frac{d \ln \sigma(M, z)}{dM} \exp \left[-\frac{\delta_c^2(z)}{2\sigma^2(M, z)} \right], \quad (35)$$

where ρ_{m0} is the present matter density of the universe and $\delta_c(z)$ is the linearly extrapolated density threshold above which structures collapse, *i.e.*, $\delta_c(z) = \delta_{lin}(z = z_{col})$.

The quantity:

$$\sigma(M, z) = D(z)\sigma_M \quad (36)$$

is the linear theory *rms* density fluctuation in spheres of comoving radius R containing the mass M , where $D(z) \equiv \delta_m(z)/\delta_m(z=0)$ is the linear growth function obtained from Eq. (29). The smoothing scale R is often specified by the mass within the volume

defined by the window function at the present time, see *e.g.* [44]. In our analysis we use the fit given by [23]:

$$\sigma_M = \sigma_8 \left(\frac{M}{M_8} \right)^{-\gamma(M)/3}, \quad (37)$$

where $M_8 = 6 \times 10^{14} \Omega_M^{(0)} h^{-1} M_\odot$ is the mass inside a sphere of radius $R_8 = 8 h^{-1} \text{Mpc}$, and σ_8 is the variance of the over-density field smoothed on a scale of size R_8 . The index γ is a function of the mass scale and the so-called shape parameter, $\Gamma = \Omega_M^{(0)} h e^{-\Omega_b - \Omega_b/\Omega_M^{(0)}}$ ($\Omega_b = 0.05$ is the baryonic density parameter) [23]:

$$\gamma(M) = (0.3 \Gamma + 0.2) \left[2.92 + \frac{1}{3} \log \left(\frac{M}{M_8} \right) \right]. \quad (38)$$

For a fixed σ_8 (power spectrum normalization) the predicted number density of dark matter halos given by the above formula is uniquely affected by the dark energy models through the ratio $\delta_c(z)/D(z)$. In order to compare the different models, we will normalize to mass function to the same value today, that is, we will require:

$$\sigma_{8,Mod} = \frac{\delta_{c,Mod}(z=0)}{\delta_{c,\Lambda}(z=0)} \sigma_{8,\Lambda}, \quad (39)$$

where the label *Mod* indicates a given model and we use $\sigma_{8,\Lambda} = 0.76$ [6].

The effect of dark energy on the number of dark matter halos is studied by computing two quantities. The first one is the all sky number of halos per unit of redshift, in a given mass bin:

$$\mathcal{N}^{\text{bin}} \equiv \frac{dN}{dz} = \int_{4\pi} d\Omega \int_{M_{\text{inf}}}^{M_{\text{sup}}} \frac{dn}{dM} \frac{dV}{dz d\Omega} dM, \quad (40)$$

where the comoving volume element is given by:

$$\frac{dV(z)}{dz d\Omega} = r^2(z)/H(z), \quad (41)$$

where $r(z) = \int_0^z H^{-1}(x) dx$ is the comoving distance. Note that the comoving volume element depends only on the cosmological background and is identical for models with and without perturbations in dark energy. The differences in the number counts when one includes dark energy clumping are due to modifications in $\delta_c(z)$ and $D(z)$.

The second quantity we compute is the all sky integrated number counts above a given mass threshold, M_{inf} , and up to redshift z [16]:

$$N(z, M > M_{\text{inf}}) = \int_{4\pi} d\Omega \int_{M_{\text{inf}}}^{\infty} \int_0^z \frac{dn}{dM} \frac{dV}{dz' d\Omega} dM dz'. \quad (42)$$

Our knowledge of both these quantities for galaxy clusters will improve enormously with upcoming cluster surveys operating at different wavebands, such as the South Pole Telescope [45].

We can now examine the modifications caused by a clustering dark energy component on the number of dark matter halos with the same observable computed in the standard ΛCDM model. First we show how the different equations of state

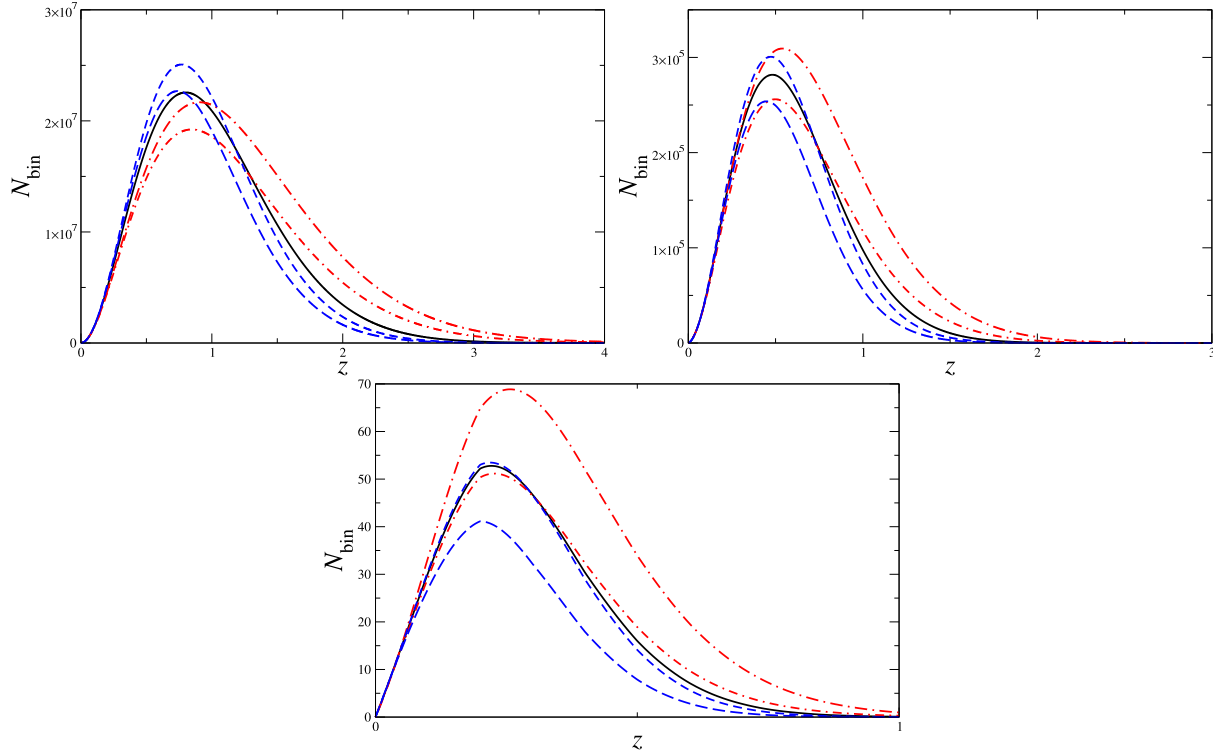


Figure 7. Evolution of number counts in mass bins with redshift for objects with masses within the range $10^{13} < M/(h^{-1}M_{\odot}) < 10^{14}$ (top left panel), $10^{14} < M/(h^{-1}M_{\odot}) < 10^{15}$ (top right panel) and $10^{15} < M/(h^{-1}M_{\odot}) < 10^{16}$ (bottom panel). The solid line corresponds to the fiducial Λ CDM result. The number counts including dark energy perturbations are shown for non-phantom (long dot-dashed line) and phantom (long dashed line) models. The results without the inclusion of dark energy perturbations are also shown for non-phantom (dot-dashed line) and phantom (dashed line) models.

impact the number of dark matter halos in given mass bins $[M_{\text{inf}}, M_{\text{sup}}]$ typical of the present-day cosmological structures, namely $[10^{13}, 10^{14}]h^{-1}M_{\odot}$, $[10^{14}, 10^{15}]h^{-1}M_{\odot}$ and $[10^{15}, 10^{16}]h^{-1}M_{\odot}$. The number counts in mass bins, $\mathcal{N}^{\text{bin}} = dN/dz$, obtained from (40), are shown in Fig. 7. In each panel we plot the actual number counts together with the number counts computed for a fiducial Λ CDM model (solid lines), for each mass bin. Notice that the more massive structures are less abundant and form at later times, as it should be in the hierarchical model of structure formation. There is a slight shift of the peak redshift for structure formation in the distinct dark energy models considered. The differences with respect to the Λ CDM model become more significant in the bins with larger masses – but, of course, given the small number of such massive objects, the uncertainty due to shot noise also becomes increasingly important.

Another important observable quantity is the integrated number of collapsed structures above a given mass, Eq. (42). We present results for the integrated number counts of structures with masses above $10^{13}h^{-1}M_{\odot}$, $10^{14}h^{-1}M_{\odot}$, and $10^{15}h^{-1}M_{\odot}$ (we cut-off the integration at $M_{\text{sup}} = 10^{18}h^{-1}M_{\odot}$, as such gigantic structures could not in practice be resolved today.) The results are displayed in Fig. 8, always compared with

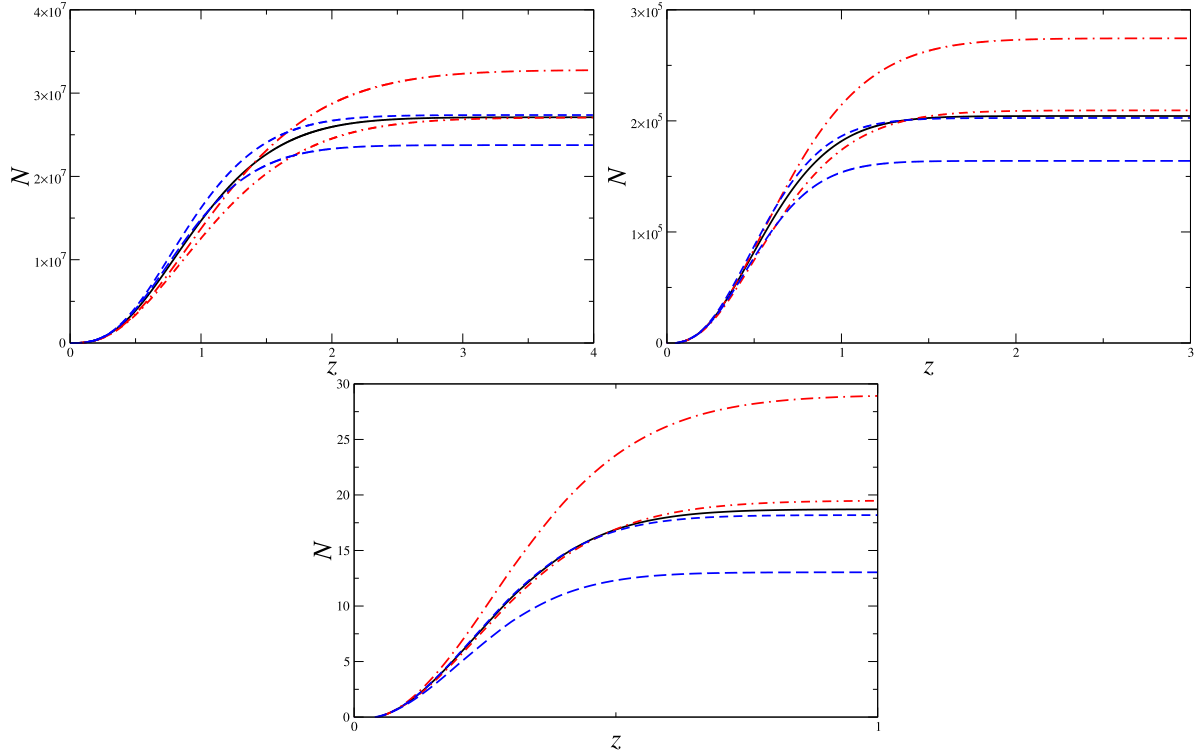


Figure 8. Evolution of the integrated number counts up to redshift z for objects with $M > 10^{13}h^{-1}M_{\odot}$ (top left panel), $M > 10^{14}h^{-1}M_{\odot}$ (top right panel) and $M > 10^{15}h^{-1}M_{\odot}$ (bottom panel). The lines correspond to the same cases as in Fig. 7.

the results for the fiducial Λ CDM model (solid lines.) Notice that the integrated number has a plateau that reflects the epoch of structure formation for a given mass. In other words, there is no formation of structures with mass above $10^{13}h^{-1}M_{\odot}$, $10^{14}h^{-1}M_{\odot}$, and $10^{15}h^{-1}M_{\odot}$ for redshifts roughly above $z = 2$, 1.5 and 0.7 , respectively. Again we find large differences compared to the Λ CDM model when dark energy perturbations are included.

6. Conclusions

Our main goal in this paper was to study the effects of including dark energy perturbations in the evolution of matter perturbations in the linear and in the non-linear regimes. Since we do not know what dark energy really is, we developed a formalism whereby we can directly use a parametrization of its equation of state in order to address this issue.

We have shown that the spherical collapse and the pseudo-newtonian approaches to the study the non-linear evolution of dark matter and dark energy perturbations are equivalent when one adopts an effective speed of sound $c_{\text{eff}}^2 = w$. In the language of spherical collapse, this is equivalent to assuming that the equation of state is the same inside and outside the collapsed region.

We found distinct behaviours in the evolution of the dark matter perturbations

for phantom and non-phantom forms of dark energy. Inclusion of dark energy perturbations inhibits the growth of dark matter perturbations for the non-phantom case but it enhances this growth in the phantom case. The reason is that dark matter overdensities lead to dark energy overdensities in the non-phantom case, but they lead to underdensities in the phantom case. Due to its gravitationally repulsive nature, dark energy overdensities inhibit, while dark energy underdensities help, the growth of dark matter perturbations.

This effect is small in the linear regime but becomes dramatic when studying the collapsed regions that have formed more recently. In particular, we found a large modification in the critical density $\delta_c(z)$ even for moderately low redshifts.

We used the Press-Schechter formalism to estimate the modifications due to dark energy perturbations in observational quantities such as number counts of galaxy clusters, which reflect the formation and distribution of dark matter halos. We found that there are large deviations compared to the standard Λ CDM model, which are more significant for the larger structures. We expect that these large deviations are a general consequence of taking into account the non-linear dark energy perturbations that are gravitationally coupled to the dark matter perturbations.

Although our use of the EoS to describe dark energy perturbations clearly constitutes a particular case, our choice was guided by the equivalence between the SC and PN approaches. However, we believe that more general models can still be described consistently in both approaches [46]. Hopefully future data on number counts of galaxy clusters will be able to discriminate among different models of dark energy.

Acknowledgments

We would like to thank C. Quercellini, T. Padmanabhan and I. Waga for useful comments. LL is supported by a CAPES doctoral fellowship; RCB thanks FAPESP for a doctoral fellowship. The works of LRA and RR are partially supported by research grants and fellowships from CNPq, and by a research grant from FAPESP (Proc. 04/13668-0.)

Appendix A.

In this paper we have analyzed the non-linear evolution of dark energy and dark matter perturbations using the PN. One can ask about the validity of such a model when pressure is taken into account. Here we explicitly show that, up to linear order, pseudo-newtonian equations are in good agreement with general relativity perturbation theory.

The relativistic equation for the gauge invariant perturbation, for a single perfect fluid can be written as [47]:

$$\ddot{\delta} + 2H \left[1 - 3 \left(w - \frac{c_s^2}{2} \right) \right] \dot{\delta} + \frac{3H^2}{2} (3w^2 - 8w - 1 + 6c_s^2) \delta = -\frac{k^2}{a^2} c_{\text{eff}}^2 \delta. \quad (\text{A.1})$$

Neglecting the term on RHS, which can be understood as a large scale approximation

or a top-hat profile, and taking $w = \text{const} = c_s^2$ we have:

$$\ddot{\delta} + 2H \left[1 - \frac{3w}{2} \right] \dot{\delta} + \frac{3H^2}{2} (3w^2 - 2w - 1) \delta = 0 , \quad (\text{A.2})$$

using $H = 2/3(1+w)t$:

$$\ddot{\delta} + \frac{4-6w}{3(1+w)} \frac{\dot{\delta}}{t} + \frac{6w^2-4w-2}{3(1+w)^2} \frac{\delta}{t^2} = 0 . \quad (\text{A.3})$$

The solution to the relativistic equation above can be written as:

$$\delta = C_+ t^{2(1+3w)/3(1+w)} + C_- t^{-1+2w/1+w} . \quad (\text{A.4})$$

In PN, Eq. (25), up to linear terms, with $c_{\text{eff}}^2 = w = \text{const}$ and δ_{PN} with no spatial dependence, is written as:

$$\ddot{\delta}_{PN} + 2H\dot{\delta}_{PN} - \frac{3H^2}{2} (1+w)(1+3w) \delta_{PN} = 0 . \quad (\text{A.5})$$

and its solution is:

$$\delta_{PN} = C_+ t^{2(1+3w)/3(1+w)} + C_- t^{-1} . \quad (\text{A.6})$$

The relativistic and pseudo-newtonian solutions differ only in the decaying mode. Note that for dust, $w = 0$, the two solutions coincide, even for the SC model [21, 48, 49]. Although both theories seem to be in good agreement, we must be watchful of phantom models. In this case the usual relativistic decaying mode $\sim t^{-1+2w/1+w}$ becomes a growing mode, while in PN it is always decaying. This behaviour is expected when phantom dark energy starts to dominate and shows that growing perturbations phantom dark energy increase the gravitational potential, unlike one should expect from a homogeneous phantom dark energy model. For all other values of $-1 < w \leq 1$ the relativistic solution $\sim t^{-1+2w/1+w}$ is a decaying mode. Hence, if the sub-dominant mode is not irrelevant for some reason, then the PN may not be reliable for phantom models at times when dark energy is strongly dominating the background evolution, i.e, $\Omega_{\text{de}} \approx 1$. Fortunately, this situation does not arise in our study.

References

- [1] Supernova Cosmology Project, R. A. Knop *et al.*, *Astrophys. J.* **598**, 102 (2003), astro-ph/0309368.
- [2] Supernova Search Team, A. G. Riess *et al.*, *Astrophys. J.* **607**, 665 (2004), astro-ph/0402512.
- [3] The SNLS, P. Astier *et al.*, *Astron. Astrophys.* **447**, 31 (2006), astro-ph/0510447.
- [4] W. M. Wood-Vasey *et al.*, (2007), astro-ph/0701041.
- [5] WMAP, D. N. Spergel *et al.*, *Astrophys. J. Suppl.* **148**, 175 (2003), astro-ph/0302209.
- [6] WMAP, D. N. Spergel *et al.*, (2006), astro-ph/0603449.
- [7] SDSS, M. Tegmark *et al.*, *Astrophys. J.* **606**, 702 (2004), astro-ph/0310725.
- [8] The 2dFGRS, S. Cole *et al.*, *Mon. Not. Roy. Astron. Soc.* **362**, 505 (2005), astro-ph/0501174.
- [9] SDSS, D. J. Eisenstein *et al.*, *Astrophys. J.* **633**, 560 (2005), astro-ph/0501171.
- [10] P. J. E. Peebles and B. Ratra, *Rev. Mod. Phys.* **75**, 559 (2003), astro-ph/0207347.
- [11] E. V. Linder, *Phys. Rev. Lett.* **90**, 091301 (2003), astro-ph/0208512.
- [12] V. Sahni, T. D. Saini, A. A. Starobinsky, and U. Alam, *JETP Lett.* **77**, 201 (2003), astro-ph/0201498.

- [13] U. Alam, V. Sahni, T. D. Saini, and A. A. Starobinsky, *Mon. Not. Roy. Astron. Soc.* **344**, 1057 (2003), astro-ph/0303009.
- [14] R. Lazkoz, S. Nesseris, and L. Perivolaropoulos, *JCAP* **0511**, 010 (2005), astro-ph/0503230.
- [15] L. Liberato and R. Rosenfeld, *JCAP* **0607**, 009 (2006), astro-ph/0604071.
- [16] N. J. Nunes and D. F. Mota, *Mon. Not. Roy. Astron. Soc.* **368**, 751 (2006), astro-ph/0409481.
- [17] M. Manera and D. F. Mota, *Mon. Not. Roy. Astron. Soc.* **371**, 1373 (2006), astro-ph/0504519.
- [18] N. J. Nunes, A. C. da Silva, and N. Aghanim, *Astron. Astroph.* **450**, 899 (2005), astro-ph/0506043.
- [19] S. Dutta and I. Maor, *Phys. Rev.* **D75**, 063507 (2007), gr-qc/0612027.
- [20] J. E. Gunn and I. Gott, J. Richard, *Astrophys. J.* **176**, 1 (1972).
- [21] E. Gaztanaga and J. A. Lobo, *Astrophys. J.* **548**, 47 (2001), astro-ph/0003129.
- [22] O. Lahav, P. B. Lilje, J. R. Primack, and M. J. Rees, *Mon. Not. Roy. Astron. Soc.* **251**, 128 (1991).
- [23] P. T. P. Viana and A. R. Liddle, *Mon. Not. Roy. Astron. Soc.* **281**, 323 (1996), astro-ph/9511007.
- [24] L.-M. Wang and P. J. Steinhardt, *Astrophys. J.* **508**, 483 (1998), astro-ph/9804015.
- [25] E. L. Lokas and Y. Hoffman, (2001), astro-ph/0108283.
- [26] S. Basilakos, *Astrophys. J.* **590**, 636 (2003), astro-ph/0303112.
- [27] W. J. Percival, *Astron. Astrophys.* **443**, 819 (2005), astro-ph/0508156.
- [28] C. Horellou and J. Berge, *Mon. Not. Roy. Astron. Soc.* **360**, 1393 (2005), astro-ph/0504465.
- [29] I. Maor and O. Lahav, *JCAP* **0507**, 003 (2005), astro-ph/0505308.
- [30] D. F. Mota and C. van de Bruck, *Astron. Astrophys.* **421**, 71 (2004), astro-ph/0401504.
- [31] Z.-K. Guo, N. Ohta, and Y.-Z. Zhang, *Phys. Rev.* **D72**, 023504 (2005), astro-ph/0505253.
- [32] R. Rosenfeld, *Phys. Rev.* **D75**, 083509 (2007), astro-ph/0701213.
- [33] J. A. S. Lima, V. Zanchin, and R. H. Brandenberger, *Mon. Not. Roy. Astron. Soc.* **291**, L1 (1997), astro-ph/9612166.
- [34] J.-c. Hwang and H. Noh, *Gen. Rel. Grav.* **31**, 1131 (1999), astro-ph/9907063.
- [35] R. R. R. Reis, *Phys. Rev.* **D67**, 087301 (2003), Erratum *ibid.* **D68**, 089901 (2003).
- [36] J. Garriga and V. F. Mukhanov, *Phys. Lett.* **B458**, 219 (1999), hep-th/9904176.
- [37] A. Vikman, *Phys. Rev.* **D71**, 023515 (2005), astro-ph/0407107.
- [38] M. Chevallier and D. Polarski, *Int. J. Mod. Phys.* **D10**, 213 (2001), gr-qc/0009008.
- [39] Y. Wang and P. Mukherjee, astro-ph/0703780.
- [40] E. L. Wright, astro-ph/0701584.
- [41] W. H. Press and P. Schechter, *Astrophys. J.* **187**, 425 (1974).
- [42] R. K. Sheth, H. J. Mo, and G. Tormen, *Mon. Not. Roy. Astron. Soc.* **323**, 1 (2001), astro-ph/9907024.
- [43] J. A. Peacock, *Cosmological Physics* (New York: Cambridge University Press, 1999).
- [44] P. J. E. Peebles, Princeton, USA: Univ. Pr. (1993) 718 p.
- [45] The SPT, J. E. Ruhl *et al.*, (2004), astro-ph/0411122.
- [46] L. R. Abramo, R. C. Batista, L. Liberato, and R. Rosenfeld, work in progress.
- [47] H. Kodama and M. Sasaki, *Prog. Theor. Phys. Suppl.* **78**, 1 (1984).
- [48] P. Fosalba and E. Gaztanaga, *Mon. Not. Roy. Astron. Soc.* **301**, 503 (1998), astro-ph/9712095.
- [49] J.-c. Hwang and H. Noh, *Gen. Rel. Grav.* **38**, 703 (2006), astro-ph/0512636.